



Fabrication and application of highly ordered mesoporous Co_3O_4 , NiO, and their metals

Geon J. Kim, Xiao-Feng Guo*

Department of Chemical Engineering, Inha University, Incheon 402-751, Republic of Korea

ARTICLE INFO

Article history:

Received 26 May 2009

Accepted 10 November 2009

Keywords:

A. Metals

A. Nanostructures

A. Oxides

D. Surface properties

ABSTRACT

Highly ordered mesoporous Co_3O_4 , NiO, and their metals were synthesized by nanocasting method using their corresponding mesoporous SBA-15 silica as a template. The obtained porous metal oxides have high surface areas, large pore volume, and a narrow pore size distribution. The N_2 -adsorption data for mesoporous metal oxides have provided the BET area of $257.7 \text{ m}^2 \text{ g}^{-1}$ and the total pore volume of $0.46 \text{ cm}^3 \text{ g}^{-1}$. The mesoporous metals were employed as a catalyst in the synthesis of (S)-3-pyrrolidinol from chiral (S)-4-chloro-3-hydroxybutyronitrile, and a high yield to (S)-3-pyrrolidinol-salt was obtained on the mesoporous Co metal catalyst.

© 2009 Elsevier Ltd. All rights reserved.

1. Introduction

For the preparation of ordered nanostructure arrays, a hard template has some advantages when compared with a soft template, especially in its specific topological stability, veracity, predictability, and controllability. Supramolecular templated mesoporous silica materials have drawn more and more attention because of their uniform mesocavities (2–30 nm), large surface areas, and large pore volumes, which make them perfect candidates to serve as hard templates. Despite considerable progress in the field of porous solids, major challenges remain in the synthesis of ordered mesoporous materials with high metal content from the coassembly of macromolecular surfactants and inorganic species. Controlling the structure of metals at the mesoscale (2–50 nm) is crucial for the development of improved fuel cell electrodes and may also assist in the miniaturization of optical and electronic materials for data transmission, storage, and computation [1,2]. An early route to preparing mesoporous metals involves the dealloying of a less noble metal from a bimetallic alloy such as Raney nickel and other metals [3]. Dealloying processes provide limited control over structural parameters such as pore geometry and order. In contrast, block copolymer self-assembly or templating with metal species provides access to highly ordered structures. The nanostructured materials have received considerable attention because of their novel size- and shape-dependent electronic, magnetic, optical, and catalytic properties that differ drastically from those of bulk

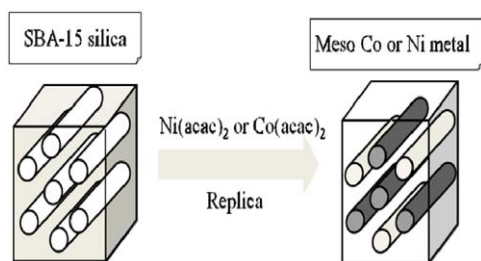
materials [4], and current research efforts are focused on the preparation of nanomaterials with new morphologies [5]. Metals with designed two-dimensional (2D) or three-dimensional (3D) nanostructures, in particular, are expected to find useful applications in [6]. A variety of synthetic pathways has been proposed for the development of nanostructure because of their numerous potential applications. Though various metal and semiconductor nanostructures have successfully been exploited, uniform mesostructured crystallized metal patterns are rarely reported. In this respect, a general synthetic strategy for mesostructured metal guided by host–guest chemistry is much desired. We have fabricated ordered mesoporous metal (OMM) replica with hexagonally ordered mesopore channels (SBA-15), designated as Co-SBA-15 and Ni-SBA-15, by using ordered mesoporous silica (OMS) as a mold in this study (Scheme 1). Mesoporous metal was employed as a catalyst for the synthesis of chiral (S)-3-pyrrolidinol-HCl by the hydrogenation of (S)-4-chloro-3-hydroxybutyronitrile. In the catalytic reduction, the mesoporous metal with one-dimensional mesopores showed a higher activity than bulk metal.

2. Experimental

2.1. Synthesis of ordered mesoporous metal oxide and metal replica using SBA-15 as template

A high quality SBA-15 was prepared using the triblock copolymer Pluronic P123 (Aldrich) as a surfactant and tetraethylorthosilicate (TEOS, 98%, Aldrich) as a silica source, modifying the synthetic procedure reported by Zhao et al. [7]. The

* Corresponding author. Tel.: +82 32 860 7472; fax: +82 32 872 4046.
E-mail address: guoxiaofeng1088@hotmail.com (X.-F. Guo).



Scheme 1. Synthesis of mesoporous metal replica.

starting composition in molar ratio for the synthesis of high grade SBA-15 was fixed as 1.72P123:0.1TEOS:0.6HCl:20H₂O. Into the calcined SBA-15, the solution of cobalt(II) acetylacetonate (Co(acac)₂, 97%, Aldrich) and nickel(II) acetylacetonate (Ni(acac)₂, 97%, Aldrich) dissolved in acetic acid and THF, respectively. As a typical method, 1 g of SBA-15 was added to a solution obtained by dissolving 0.6 g of Co(acac)₂ or Ni(acac)₂ in acetic acid (2.5 mL) or THF (2.5 mL). The mixture was evaporated to remove the solvent by heating at 393 K. The sample turned to a brown or yellow color during the treatment. The silica composite sample was treated thermally by following the same procedure as mentioned above at 373 and 433 K after additional impregnation of 0.6 g of Co(acac)₂ or Ni(acac)₂ in acetic acid (2.5 mL) or THF (2.5 mL). The sample was calcined at 550 °C for 5 h (1 °C/min). The mesoporous metal oxide was obtained by refluxing in 2 M NaOH for 2 h to remove the silica template. The template-free mesoporous metal oxides were designated as Co₃O₄-SBA-15 and NiO-SBA-15. Mesoporous oxides were reduced to their corresponding metal with H₂ flow through the reactor while temperature was kept at 350 °C for 6 h. The powder metal product was obtained and designated as Co-SBA-15 and Ni-SBA-15, respectively.

2.2. Characterization

X-ray powder diffraction (XRD) data of parent SBA-15 and its corresponding replica (Co₃O₄ or NiO-SBA-15, and Co-SBA-15 or Ni-SBA-15) were acquired on a D/MAX 2500V/PC diffractometer using CuK α radiation. The morphology and microstructures of as-prepared samples were characterized by field emission transmission electron microscopy (FE-TEM, S-4200) and field emission scanning electron microscopy (FE-SEM, JEM-2100F). The nitrogen adsorption/desorption analysis was performed at –196 °C by using a surface area and porosity analyzer equipment (Micromeritics, ASAP 2010). The specific surface areas were calculated according to the BET theory, and the mean pore size was determined by BJH analysis.

2.3. Typical procedure for (S)-3-pyrrolidinol-salt

After dissolution of 4 g of (S)-4-chloro-3-hydroxybutyro-nitrile in 40 mL of methanol, 0.5 mg of mesoporous metal was added to that solution. The mixture was stirred under a hydrogen pressure of 8 kg/cm² at room temperature for 36 h in the autoclave reactor. The solvent was evaporated finally to give a (S)-3-pyrrolidinol-HCl salt. The yield of product was determined from the weight of isolated salt.

3. Results and discussion

The formation of mesopores in Co₃O₄-SBA-15, NiO-SBA-15, Co-SBA-15, and Ni-SBA-15 was determined by XRD, TEM, and N₂

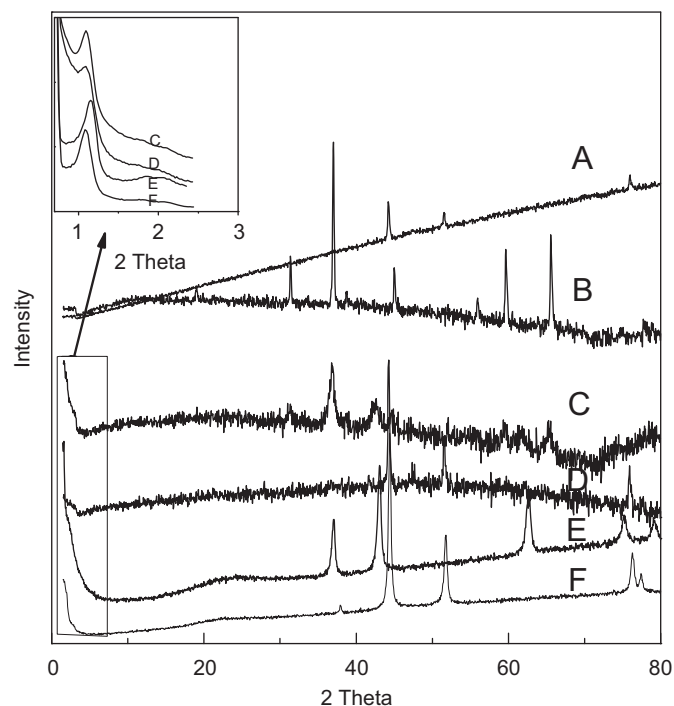


Fig. 1. X-ray diffraction patterns of bulk Co (A); bulk Co₃O₄ (B); Co₃O₄-SBA-15 (C); Co-SBA-15 (D); NiO-SBA-15 (E); and Ni-SBA-15 (F).

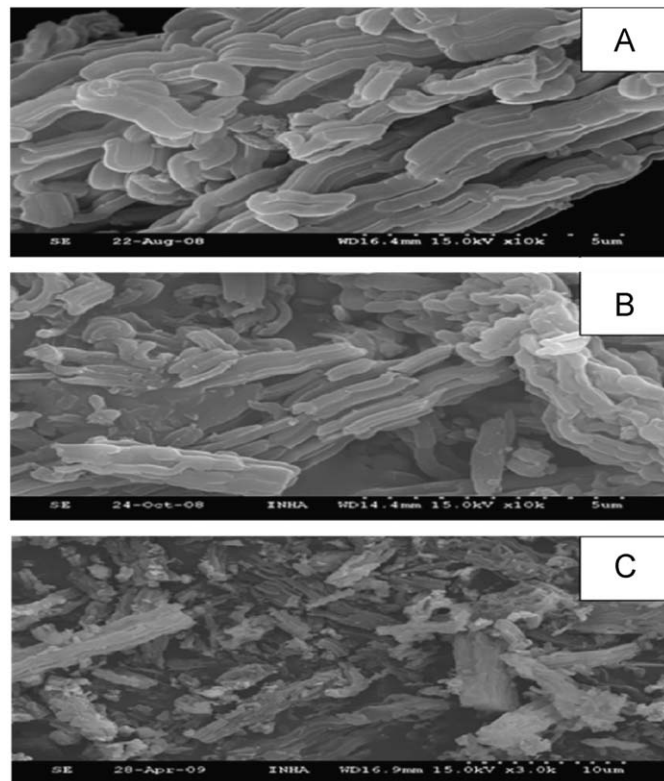


Fig. 2. Scanning electron microscopy images of SBA-15 in low magnification (A); Ni-SBA-15 in high magnification (B); and Co-SBA-15 in high magnification (C).

adsorption analysis. The wide-angle-X-ray diffraction (WAXRD) results show characteristic peaks that can be indexed as Co₃O₄, NiO, Co, and Ni crystalline phase and ordered mesophase (Fig. 1). X-ray-diffraction (XRD) clearly shows characteristic peaks that the ordered arrangement of mesopore in the synthesized replica

gives rise to the well-resolved XRD peaks as shown in Fig. 1, which can be assigned to (1 0 0), (1 1 0), and (2 0 0) diffractions of the 2D hexagonal space group (p6mm). The XRD results showed that the OMM replicas fabricated from ordered mesoporous SBA-15 in this work exhibited well-developed regular mesoporous channels.

FE-SEM images revealed that the as-synthesized mesoporous metal consists of many rope-like domains with relatively uniform sizes of $\sim 2 \mu\text{m}$, which are aggregated into wheat-like macrostructures. Both Co-SBA-15 and Ni-SBA-15 replica have exhibited the same morphological feature as compared to the corresponding parent SBA-15 silica mold (Fig. 2). This result indicates that the introduction of $\text{Co}(\text{acac})_2$ or $\text{Ni}(\text{acac})_2$ to form the metal oxide

wall was successfully performed in the whole range of mesopores of starting SBA-15 silica.

To analyze the pore geometry and structure of ordered mesoporous oxides, BJH analyses were performed to measure the N_2 adsorption branch corresponding to the equilibrium (Fig. 3). N_2 adsorption/desorption isotherm of calcined original SBA-15 (Fig. 3A) was the H1-type hysteresis loop that is typical for mesoporous materials with ordered cylindrical channels.

However, the mesoporous metal oxide showed a hysteresis curve corresponding to the cylinder-like mesopore channels (Fig. 3B and 3C). The N_2 -adsorption data for Co_3O_4 -SBA-15 have provided a BET area of $257.8 \text{ m}^2 \text{ g}^{-1}$ and a pore volume of $0.46 \text{ cm}^3 \text{ g}^{-1}$. The latter can be related to the volume of the ordered mesopores primarily, with minor contribution of micropores. The NiO-SBA-15 also exhibited a very high adsorption amount of nitrogen. The NiO-SBA-15 sample gave a BET area of $256.7 \text{ m}^2 \text{ g}^{-1}$ and a pore volume of $0.50 \text{ cm}^3 \text{ g}^{-1}$. The N_2 adsorption result also indicates that Co_3O_4 -SBA-15 had a quite narrow pore-size distribution of 7.1 nm, while the pore size distribution for SBA-15 silica was centered at 7.2 nm. The mean pore size of NiO-SBA-15 was 6.3 nm.

Fig. 4 shows the two types of FE-TEM images for Co-SBA-15 and Ni-SBA-15 viewed along or perpendicular to the direction of hexagonal pore arrangement. As can be seen in those TEM images, the mesopore structures of Co-SBA-15 and Ni-SBA-15 are exactly the inverse replica of SBA-15 silica. The TEM image at high magnifications showed the well-defined mesopore structures in ordered mesoporous metals. The metal nanorods are interconnected by spacers, which are constituted by the metal that filled the channel-interconnecting micropores within the SBA-15 wall.

In the catalytic reduction of the 4-chloro-3-hydroxy butyronitrile, metal catalysts such as Raney metal, palladium, and platinum can be used preferably to convert the cyano group into the primary amine. In this work, OMM were tested as a catalyst for the synthesis of (S)-3-pyrrolidinol-HCl salt (S-PD-salt) from the optically active (S)-4-chloro-3-hydroxybutyronitrile (S-CHB), and the results for the catalytic activity are listed in Fig. 5.

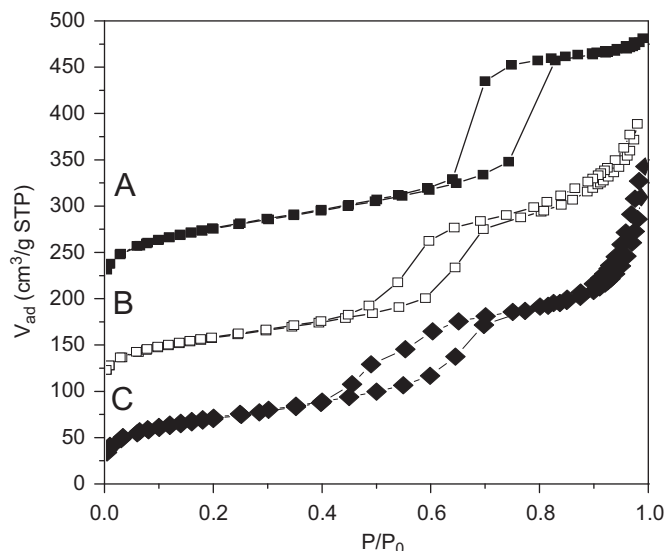


Fig. 3. N_2 adsorption/desorption isotherms for SBA-15 silica (A); Co_3O_4 -SBA-15 (B); NiO-SBA-15 (C).

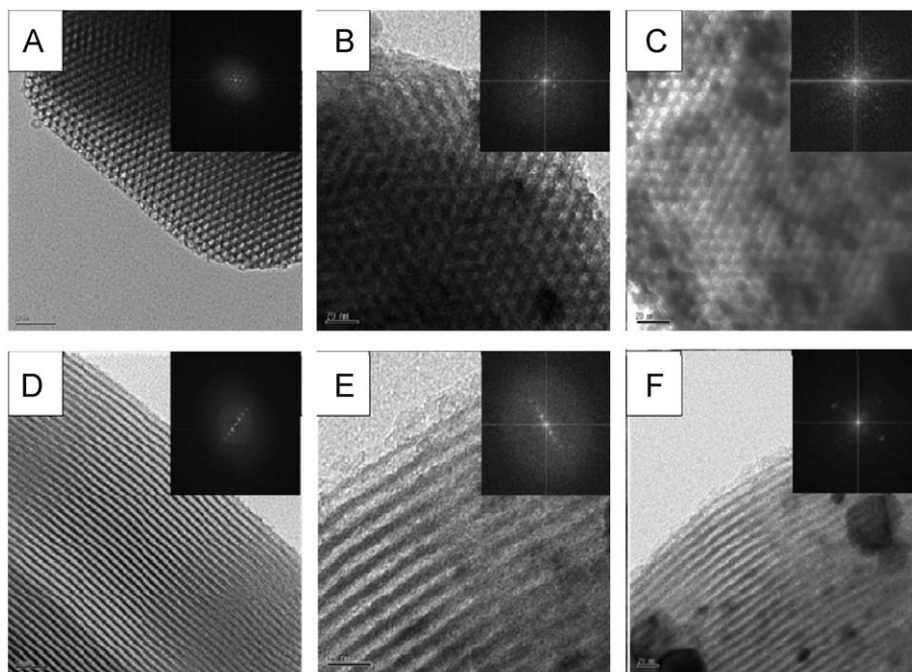


Fig. 4. TEM photographs of SBA-15 (pore entrance) (A); SBA-15 (view of side wall) (B); Ni-SBA-15 (pore entrance) (C); Ni-SBA-15 (view of side wall) (D); Co-SBA-15 (pore entrance) (E); and Co-SBA-15 (view of side wall) (F).

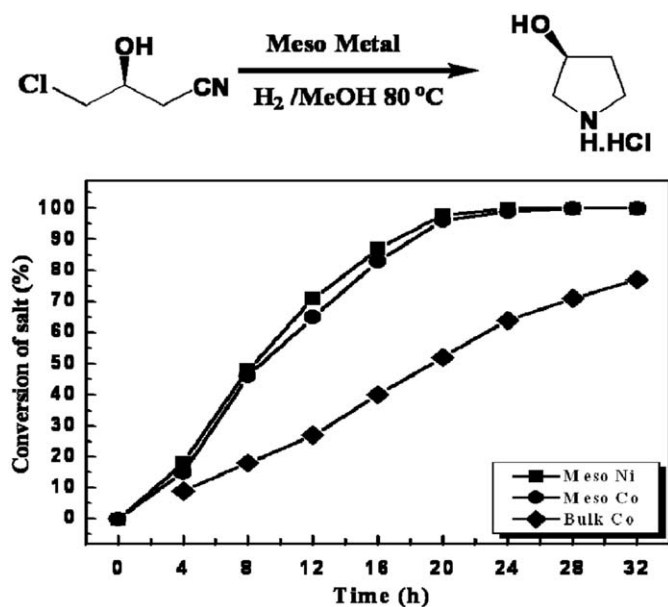


Fig. 5. Catalytic activities of mesoporous metals in the hydrogenation of chiral (S)-4-chloro-3-hydroxybutyronitrile to obtain the (S)-3-pyrrolidinol-HCl salt (H₂: 8 kg/cm²; Temp.: 80 °C).

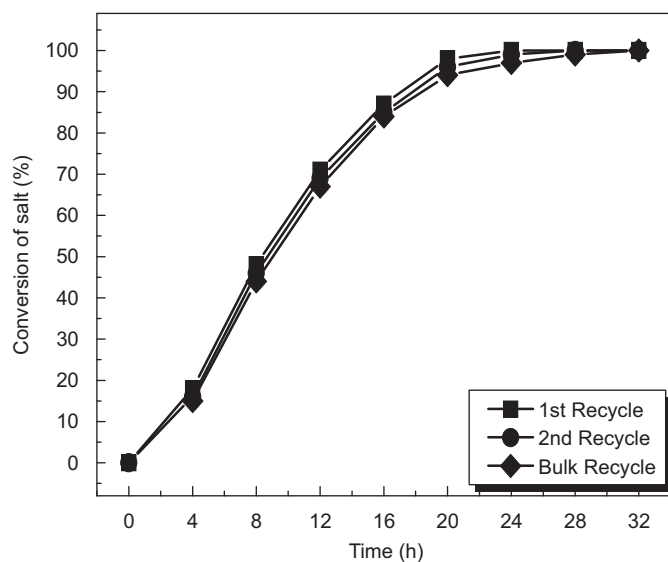


Fig. 6. The recyclability of Ni-SBA-15 in the hydrogenation of chiral (S)-4-chloro-3-hydroxybutyronitrile to obtain the (S)-3-pyrrolidinol-HCl salt (H₂: 8 atm; Temp.: 80 °C).

Accordingly the effect of support type on the product yield was determined, and the obtained results are shown in Fig. 5. The Ni-SBA-15 and Co-SBA-15 gave much higher yield to S-PD-salt than the bulk Co in the reduction of S-CHB. It was attributed to OMM with a large volume and big pore size. Mesoporous Ni showed slightly higher activity than mesoporous Co metal.

Recyclability of Ni-SBA-15 was investigated in the same reactions as mentioned above. The catalyst was collected by simple washing with MC, THF solvent for reuse after completion

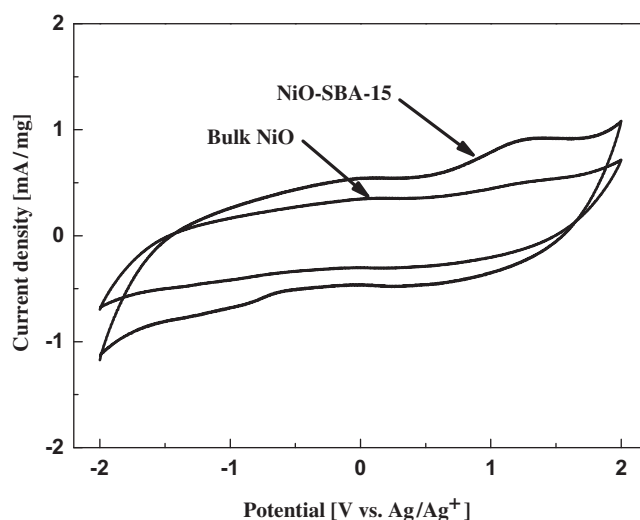


Fig. 7. Cyclic voltammograms of NiO in 0.5 M Et₄NBF₄/Propylene carbonate (PC) at 70 mV/s scan rate; loading amount of the working electrode: 5 mg/cm².

of reaction. The catalyst could be recycled efficiently, as summarized in Fig. 6. After three times reuse, catalysts retained the high activity, but a low decrease in yield was found by repeated use, indicating the slight loss.

Mesoporous nickel oxide electrodes were used in the electrochemical capacitor and their performance was tested using cyclic voltammetry (CV) as indicated in Fig. 7. The high porosity and large pore size of films allow for easy access of the redox process and results in high packing density of the active material. Such type of porous materials leads to a high surface specific area and porous volume, which provide the structural foundation for the high specific capacitance.

4. Conclusions

The OMM such as Ni-SBA-15 and Co-SBA-15 have been synthesized by nanocasting method using their corresponding mesoporous silicas as a mold. The obtained NiO-SBA-15 and Co₃O₄-SBA-15 have the high surface area with a narrow pore size distribution, exhibiting BET area of 257.8 m² g⁻¹ and a total pore volume of 0.46 cm³ g⁻¹. The OMM were employed in the synthesis of (S)-3-pyrrolidinol-salt from chiral (S)-4-chloro-3-hydroxybutyronitrile. It was investigated that the OMM are efficient for the hydrogenation of cyano groups to amine, and higher activity was obtained by nanocasting method than bulk metal.

References

- [1] A. Haryono, W.H. Binder, *Small* 2 (2006) 600–611.
- [2] A.C. Balazs, T. Emrick, T.P. Russell, *Science* 314 (2006) 1107–1110.
- [3] M. Raney, U.S. Patent 1628190, 1927.
- [4] G. Schmid, *Chem. Rev.* 92 (1992) 1709–1927.
- [5] G.R. Patzke, F. Krumeich, R. Nesper, *Angew. Chem. Int. Ed.* 41 (2002) 2446–2461.
- [6] A. Roucoux, J. Schulz, H. Patin, *Chem. Rev.* 102 (2002) 3757–3778.
- [7] D. Zhao, Q. Huo, J. Feng, B.F. Chmelka, G.D. Stucky, *J. Am. Chem. Soc.* 120 (1998) 6036–6042.